

## CURRENT TRANSPORT MECHANISM IN PRINTED AG THICK FILM CONTACTS TO AN N-TYPE EMITTER OF A CRYSTALLINE SILICON SOLAR CELL

Gunnar Schubert, Frank Huster, Peter Fath

University of Konstanz, Department of Physics, P.O. Box X916, D-78457 Konstanz, Germany  
Phone: ++49-7531-88-2088, Fax: ++49-7531-88-3895. Email: Gunnar.Schubert@uni-konstanz.de

**ABSTRACT:** In this contribution the electrical front contact formation in a standard industrial solar cell process is investigated. The focus is on the critical part in establishing a current path from the emitter into the silver thick film contact, the growth of silver crystallites into the silicon. It was found that during firing silver particles dissolve in liquid lead, resulting from the redox reaction of silicon with PbO contained in the glass. [100]-planes of silicon dissolve in turn in the liquid silver – lead phase, so that inverted pyramids are etched. On cooling down, silver recrystallizes preferably on [111]-planes of the pyramids. These results led to a model that explains the formation of silver – silicon contacts in thick film firing processes. Additionally, a measurement method is introduced which provides in-situ contact resistance measurements during the firing process. Results on n-type samples suggest that electrical contact formation depends on the cooling sequence of a firing cycle.

**Keywords:** silicon solar cell, thick film metallization, front contact

### 1. INTRODUCTION

The  $n^+$  emitter of an industrial crystalline silicon solar cell is predominately contacted by silver (Ag) based thick film pastes. The paste, consisting of an organic binder system, silver particles and glass powder, is usually screen-printed on the antireflection coating of the cell, dried and fired through the dielectric layer in an IR-belt furnace which provides fast firing sequences with high ramp up rates ( $>20\text{K/s}$ ). The peak temperature of the cell during firing is usually below  $835^\circ\text{C}$ , the eutectic temperature in the silver – silicon system [1]. In this process the glass frit plays the most important role. It etches through the dielectric layer to enable electrical contact to the emitter of the solar cell. Consequently a glass layer accumulates on the silicon surface. The glass frit is therefore supposed to affect the current transport from the emitter into the silver thick film to a great extent. Being advantageous in many aspects the weak point of the silver thick film contact is still the necessity of a highly doped emitter ( $R_{\text{sheet}} = 35\text{-}55\text{ Ohm/sq.}$ ,  $N_{\text{surf}} \approx 2 \cdot 10^{20}\text{ cm}^{-3}$ ) to achieve contact resistivities ( $\rho_c$ ) smaller than  $10\text{ mOhmcm}^2$  that do not affect the series resistance of the solar cell to a great extent. Further optimisation of Ag thick film pastes to allow a reasonably small  $\rho_c$  on emitters with a sheet resistance of up to  $100\text{ Ohm/sq.}$  requires detailed understanding of the electrical contact and its formation.

In the past years studies have been made to investigate the silver thick film contact in more detail [2-7]. The main focus of these investigations was on the microstructure of the formed thick film contact. Silver crystallites have been found below the contact recrystallized preferably on [111] silicon planes [3-7]. They are separated from the bulk silver of the finger by a glass layer (see Figure 1).

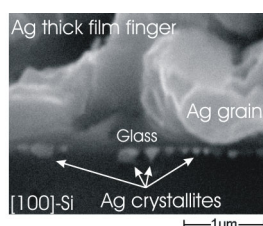


**Figure 1:** SEM-picture of the interface of a silver thick film finger on [100]-orientated silicon.

Ballif et al. [5] measured a contact resistivity of about  $0.2\text{ }\mu\text{Ohmcm}^2$  between a silver crystallite and the emitter of an industrial solar cell. Therefore, it is likely that these silver crystallites play the major role in establishing a current transport path from the emitter into the bulk of the thick film finger. Then two main questions need to be answered: 1. What is the growth mechanism of the silver crystallites? 2. What is the nature of the current transport mechanism between the crystallites and the silver finger?

In this contribution we investigated the growth mechanism of the silver crystallites using SEM, EDX, DTA and XRD analysis and present an in-situ contact resistance ( $R_c$ ) measurement setup which provides insights in the kinetics of the electrical contact formation.

### 2. IN-SITU $R_c$ MEASUREMENT

To gain insight in the temperature and time dependence of the electrical contact formation a new contact resistance ( $R_c$ ) measurement setup was established. A commercial Ag thick film paste was printed in a finger pattern on polished n-type silicon  $5 \times 5\text{ cm}^2$  substrates ( $N_D = 5 \cdot 10^{19}\text{ cm}^{-3}$ , thickness:  $380\text{ }\mu\text{m}$ ). The finger length was defined as  $1\text{ cm}$  by a sawing step. Two fingers (distance:  $2.5\text{ mm}$ , width:  $120\text{ }\mu\text{m}$ ) were contacted using a silver wire (diameter:  $25\text{ }\mu\text{m}$ ) to allow a four point measurement of the resistance  $R$  between the fingers. In Figure 2 the experimental setup is shown. During firing in a rapid thermal processing (RTP) furnace (AST SHS100) both the sample temperature and the resistance between the two fingers are measured simultaneously every  $200\text{ ms}$ . The firing profile was varied in peak temperature, peak time and ramp down rate. To confirm the in-situ measurement  $R_c$  was determined using a TLM  $R_c$  measurement setup after firing.

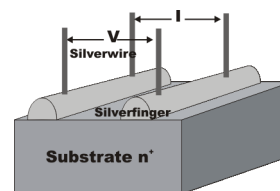


**Figure 2:** Experimental setup of the in-situ  $R_c$  measurement

In Figure 3 the total resistance  $R$  between two fingers on n-type samples during two firing profiles is presented. In both firing sequences the same ramp up rate and peak temperature were chosen. In the first case (sample 307)  $T_{\text{peak}}$  was held for 10s. After that the sample was cooled down in 4s to 700°C and in 60s to 500°C. Then heating was turned off and the sample was cooled down to room temperature. In the second case (sample 600) the peak temperature was held for 40s and the heating was turned off subsequently to ensure the fastest possible cooling rate.

In both cases the electrical contact formation started during the ramp up period. At  $T_{\text{peak}}$   $R$  reached a constant but noisy level. In the first case (slow cooling down) a large decrease in  $R$  was measured during ramp down. In contrast during fast cooling  $R$  decreased only lightly.

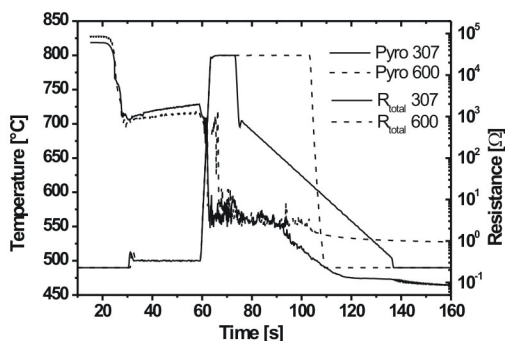


**Figure 3:** In-Situ  $R_C$  measurement on n-type samples. The used pyrometer was calibrated from 490°C to 900°C.

The slow decrease of the total resistance when cooling down from 490°C to room temperature can be explained with the temperature dependence of the sheet resistance  $R_{\text{sheet}}$ . Simulations using PC1D [8] showed that  $R_{\text{sheet}}(T)$  is dominated by the temperature dependence of the majority carrier mobility in case of a substrate doping of  $N_D = 5 \cdot 10^{19} \text{ cm}^{-3}$ .

Contact resistivity measurements after firing confirmed the values measured with the in-situ method. The total resistance between two fingers of sample 307 was between 0.01 and 0.02 Ohm. Taking into account a sheet resistance of the n-type substrate of 0.041 Ohm/sq. a contact resistivity  $\rho_c$  in the order of magnitude of  $10^{-5} \text{ Ohmcm}^2$  is calculated using the transfer length method. In contrast, on sample 600  $\rho_c = 2 - 4 \text{ mOhmcm}^2$  was determined. The results indicate that slow cooling improves the contact resistance of a silver thick film paste to a moderately phosphorous doped silicon sample. Contact resistivities with a similar order of magnitude as evaporated contacts were reached.

Applying the in-situ  $R_C$  measurement method to  $n^+$ -p diodes is in principle possible but analysis is extended. At high temperatures the number of carriers in the lowly doped p-base increases rapidly due to thermal generation. Consequently the  $p^+$ -n diode – in this measurement setup the p-base is isolated from the emitter at room temperature – is in forward bias. Therefore the temperature dependence of the specific resistivity in the base will dominate the measurement.

### 3. GROWTH MECHANISM OF SILVER CRYSTALLITES

To study the growth mechanism of the silver crystallites into the emitter of a solar cell, which are assumed to be responsible for the electrical contact between thick film paste and silicon, competing processes during contact formation were investigated separately. Three systems were analysed: pure silver on silicon, glass containing dissolved silver on silicon and a “near reality” system, a mixture of silver and glass powder on silicon.

#### 3.1 Crystal growth from non-fritted silver paste

Initially we studied the reaction between silver and silicon at  $T=900^\circ\text{C}$  well above the eutectic temperature of  $835^\circ\text{C}$ . A paste consisting only of silver powder and binder was printed on a polished [100] orientated silicon substrate and fired in a tube furnace at  $900^\circ\text{C}$  for 15min. Cross-section SEM and EDX investigations again showed silver pyramids in the silicon (see Figure 4a). This result indicates that silicon and silver starts to get fluid at  $T = T_{\text{eutectic}}$  at particular points (e.g. imperfectness in the native oxide layer or defined silver particle contact points to silicon). Silicon dissolves according to the phase diagram (Figure 4b). Obviously this dissolving process is anisotropic, so that inverted pyramids develop. On cooling down, silver recrystallizes and fills up the pyramids.

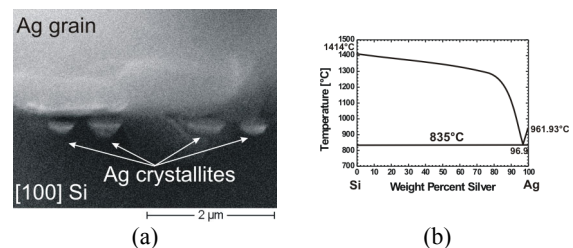


**Figure 4:** (a) SEM cross section picture of silver on [100]-orientated silicon after firing at  $900^\circ\text{C}$  for 15 min. (b) Silver-Silicon phase diagram (after [1]).

Although the resulting inverted silver pyramids are also observed in standard firing processes, the growth mechanism in this form can, however, not occur in a standard firing-through process, because the peak firing temperature of a cell is usually below  $835^\circ\text{C}$ .

#### 3.2 Crystallite growth from glass containing silver

Silver was dissolved in a lead borosilicate glass prior to depositing and firing the glass on silicon. Again, inverted silver pyramids were found to have been grown into [100]-orientated silicon but at peak temperatures of only  $800^\circ\text{C}$  [3,7]. The problem, though, is that this dissolving process is too slow to be the dominant mechanism in a typical thick film firing process. In the experiments described in [3] and [7] silver was always dissolved in the glass for at least one hour at  $1000^\circ\text{C}$  prior to depositing it on silicon. Forti et al. also showed that silver dissolving in lead borosilicate glass is a slow process [9].

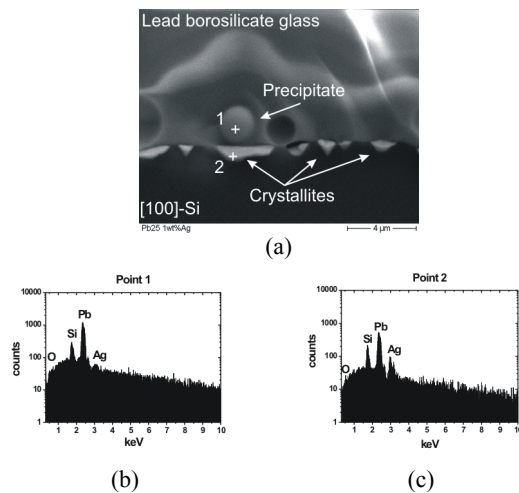


**Figure 5:** (a) SEM cross section of paste 1 on [100] silicon. (b) EDX analysis of point 1. (c) EDX analysis of point 2.

### 3.3 Crystallite growth from silver powder – glass system

Following the approach of separation of competing processes the interaction of lead borosilicate glass with silicon was investigated. It was found that this glass etches into silicon via a redox-reaction between silicon and lead oxide contained in the glass [3,10]. The temperature of the sample is, even in the early states of the firing process, above the melting point of metallic lead of 328°C [1]. Therefore the formed lead is liquid. After firing glass on silicon without any silver the [100]-orientated silicon surface below the glass does not show inverted pyramids but is corrugated [7].

To study the transport process of silver to silicon and the formation of inverted silver pyramids on [100]-orientated silicon in more detail, a set of pastes were prepared consisting of binder, lead borosilicate glass powder and an increasing amount of silver particles (paste 0: 100 wt.% glass, 0 wt.% Ag; paste 1: 1 wt.% Ag; paste 2: 5 wt.% Ag and paste 3: 10 wt.% Ag). These pastes were deposited on polished [100] silicon and fired in the RTP furnace using different parameters for ramp up, peak temperature and time and ramp down.

Figures 5a and 6a show typical SEM cross-section pictures of paste 1 and 2 respectively. The sample was fired with a heating rate of 20K/s after burn-out, a peak temperature of 800°C for 120s and a cooling rate of 1K/s. EDX analysis showed that the composition of the inverted pyramids depends on the amount of silver. If 1 wt.% silver is mixed with the glass frit, the crystals grown into the silicon consist of both lead and silver. In the precipitates above the interface the amount of lead is much higher but silver is also found (Figures 5b and 5c).

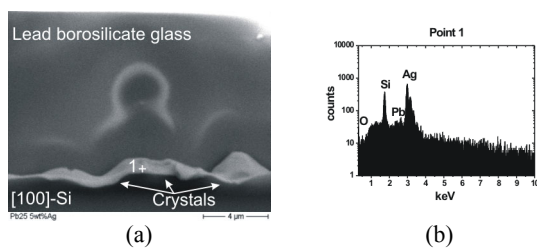


**Figure 6:** (a) SEM cross section picture of paste 2 on [100] silicon. (b) EDX analysis of point 1.

With increasing silver content the amount of silver in the crystals increases. Due to resolution limitations in the EDX analysis (rough surface, penetration depth of electron beam in specimen) the amount of lead in the crystals is not accurately quantifiable (Figure 6b). At the same time lead rich precipitates vanish. The vanishing of lead precipitates when a large amount of metallic silver is present was already described in [3] and is consistent with the TEM investigations of Ballif et al. [4].

To study the reaction behaviour during firing differential thermal analysis (DTA) was applied to a number of samples. To obtain maximum signal [100] silicon was crushed into powder and mixed with glass and silver. The used crucibles consisted of an Al<sub>2</sub>O<sub>3</sub> ceramics. An empty crucible served as reference. Every sample was heated up in air to study the reaction and the reaction products. In Figure 7a curves of two different samples of the second heating step are presented. The first sample is a mixture of glass frit and 10% silicon powder (dashed line). To the second mixture 5% silver powder was added. In case of mixture 1, the melting of lead precipitates formed during the first firing step is clearly visible (endothermic peak at T = 322°C). When adding a small amount of silver powder (mixture 2) an endothermic peak at T = 298°C is measured. This temperature can be identified as the melting temperature of a lead-silver eutectic (Figure 7b). This result together with the SEM/EDX analysis described above suggests that a silver – lead phase is formed during the firing process.

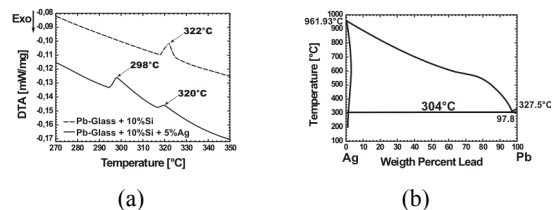


**Figure 7:** (a) DTA measurement: Second heating cycle of different mixtures. (b) Silver – Lead phase diagram (after [1]).

To test this hypothesis, a paste consisting of silver and lead oxide (10 wt.%) was mixed and fired together with a pure silver paste on polished [100] silicon (ramp up: 20K/s, T<sub>peak</sub>=800°C, t<sub>peak</sub>=120s, ramp down: 20K/s). PbO is reduced by silicon resulting in lead and silicon dioxide [11]. In Figure 8 SEM cross-section pictures are presented. No crystallites were found below the pure silver paste but below the silver lead oxide mixture. EDX measurements on crystallites confirmed that they consist mainly of silver.

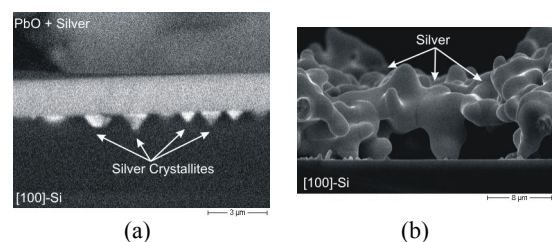


**Figure 8:** SEM cross section pictures: (a) PbO+Ag on [100] silicon. (b) pure Ag on [100] silicon.

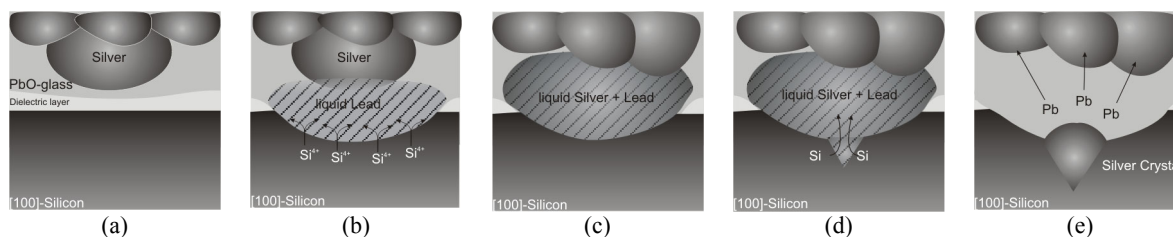


**Figure 9:** Silver growth model. (a) Schematic cross section of Ag thick film paste on [100] silicon after burn-out. (b) Glass has penetrated the dielectric layer → redox reaction between glass and silicon. (c) Silver particle dissolves in liquid lead according to phase diagram. (d) Silicon interacts with liquid silver – lead alloy → formation of inverted pyramids. (e) Phase separation on cooling down → Silver recrystallizes on [111] planes of the pyramid.

In conclusion the experiments showed that silver interacts with liquid lead resulting from the redox reaction between silicon and glass. At high temperatures the liquid lead – silver alloy interacts with silicon resulting in inverted pyramids filled with silver.

### 3.4 Discussion

Based on the results above the following microscopic model for the growth mechanism of silver crystallites in a silver thick film firing process is proposed.

Due to the etching mechanism of lead borosilicate glass with silicon, liquid lead forms during the firing process (Figure 9b). As soon as liquid lead comes into contact with silver (e.g. with small grains, located near the silicon surface) the silver particles melt to form a liquid silver – lead phase (Figure 9c). According to the phase diagram this phase consists at 800°C of approx. 72% Ag (Figure 7b). This process is very fast as simple experiments indicate. Mixtures of silver powder and lead become fluid in a reducing atmosphere (Ar-H) at temperatures between 400°C and 800°C.

The silver – lead melt is now in contact with the silicon surface. The experiments indicate that dissolving of [100] silicon planes respectively inverted pyramid formation starts at  $T > 700^\circ\text{C}$ . Lead is therefore assumed to lower the temperature of silver – silicon interaction (Figure 9d).

On cooling down, silver and lead separate according to the phase diagram. Consequently silver recrystallizes on the [111] planes of the inverted pyramid (Figure 9e). If a large amount of silver is present no lead containing precipitates were found in the glass. It is thus likely that lead is dissolved in silver, in the crystallite and/or in the bulk (see Figure 7b). This assumption is supported by X-ray diffraction measurements that were performed on different pastes (paste 0, paste 1 and paste 2) fired on [100] silicon. The intensity of the crystalline lead peaks decreased with increasing silver content.

The recrystallization process of the silicon dissolved by the lead – silver alloy is not yet clear. Obviously it does not recrystallize completely in the formed inverted pyramid. One possible mechanism is that during interaction with the silver–lead melt silicon is transported away from the pyramid. On cooling down it can recrystallize on silicon surface areas surrounding the pyramid.

The model explains the growth of silver crystallites into silicon and points out the importance of glass frit for contact formation. It also implies that the growth process of the silver crystallites and therewith the electrical contact formation can be influenced by the process parameters of contact firing. According to the results the PbO content in the glass frit plays an important role in electrical contact formation.

## 4. CONCLUSION

The investigations on the silver growth mechanism into silicon in a silver thick film firing process showed that the glass frit is the most critical part in contact formation. The results led to a model that describes silver – silicon contact formation for fast firing processes. The in-situ  $R_c$  measurement method gave first hints that direct crystallite – finger interconnections are responsible for very low contact resistivities in silver thick film contacts. Further investigations are necessary to clarify the nature of silver thick film contacts completely.

## ACKNOWLEDGEMENTS

We would like to thank B. Fischer for fruitful discussions and E. Biegger for DTA and XRD measurements. This work was supported by the EC within the EC2Contact project under project No. ENK6-CT-2001-00560.

## REFERENCES

- [1] T. B. Massalski, Binary Alloy Phase Diagrams, 2nd Edition, 1-3 (ASM International, USA, 1992)
- [2] B. Thuillier, S. Berger, J.P. Boyeaux, A. Laugier, Proc. 28<sup>th</sup> IEEE PVSC, Anchorage, (2000) 411-413
- [3] G. Schubert, B. Fischer, P. Fath, Proc. PV in Europe Conference, Rome (2002) 343-346
- [4] C. Ballif, D. M. Huljic, A. Hessler-Wyser, G. Willeke, Proc. 29<sup>th</sup> IEEE PVSC, Glasgow, 2002 360-363
- [5] C. Ballif, D. M. Huljic, G. Willeke, A. Hessler-Wyser, Appl. Phys. Lett. 82, No. 12 (2003) 1878-1880
- [6] C. Khadilkar, S. Sridharan, T. Pham, A. Shaikh, S. Kim, Proc. 14<sup>th</sup> PVSEC, Bangkok, (2004) in print
- [7] G. Schubert, F. Huster, P. Fath, Proc. 14<sup>th</sup> PVSEC, Bangkok, (2004) in print
- [8] P. A. Basore, D. A. Clugston, PC1D V5.0, University of New South Wales (1997)
- [9] B. Forti, A. F. Gualtieri, M. Leoni, M. Prudenziati, C. C. Tang, Mat. Sci. F. 321-324 (2000) 1051-1055
- [10] G. Schubert, Diploma Thesis, Departement of Physics, University of Konstanz, 2002
- [11] YaA.Ugai, P. Fertsh, IYa. Mittova, V.Z. Anokhin, T.A. Gadesbskaya, Inorganic Materials (USA), vol.13, no.9, (1977) 1304-1306